Am J Cancer Res 2023;13(8):3482-3499
www.ajcr.us /ISSN:2156-6976/ajcr0149880

Original Article

Colorectal cancer cell-secreted exosomal miRNA N-72 promotes tumor angiogenesis by targeting CLDN18

Ying Li[1,2*], Di Jiang[1*], Zhi-Xin Zhang[3], Jun-Jun Zhang[1], Hong-Yu He[4], Jian-Li Liu[1], Ting Wang[1], Xia-Xia Yang[5], Bang-Dong Liu[1], Li-Li Yang[1], Xiao Zhi[1], Xiao-Bei Zhang[6], Tian-Lun Li[1], Yan-Rong Liu[1]

[1]Department of Pathology, Affiliated Hospital of Jining Medical University, Jining Medical University, Jining, Shandong, China; [2]Postdoctoral Mobile Station of Shandong University of Traditional Chinese Medicine, Jinan, Shandong, China; [3]Department of Gastrointestinal Surgery, Affiliated Hospital of Jining Medical University, Jining, Shandong, China; [4]Department of Medical Equipment, Affiliated Hospital of Jining Medical University, Jining, Shandong, China; [5]Department of Clinical Laboratory, Affiliated Hospital of Jining Medical University, Jining Medical University, Jining, Shandong, China; [6]Medical Research Center, Affiliated Hospital of Jining Medical University, Jining, Shandong, China. [*]Equal contributors.

Received February 27, 2023; Accepted July 20, 2023; Epub August 15, 2023; Published August 30, 2023

Abstract: Angiogenesis is essential for the growth and metastasis of several malignant tumors including colorectal cancer (CRC). The molecular mechanism underlying CRC angiogenesis has not been fully elucidated. Emerging evidence indicates that secreted microRNAs (miRNAs) may mediate the intercellular communication between tumor cells and neighboring endothelial cells to regulate tumor angiogenesis. In addition, exosomes have been shown to carry and deliver miRNAs to regulate angiogenesis. miRNA N-72 is a novel miRNA that plays a regulatory role in the EGF-induced migration of human amnion mesenchymal stem cells. However, the relation between miRNA N-72 and cancer remains unclear. We here found that CRC cells could secrete miRNA N-72. A high miRNA N-72 level was detected in the serum of CRC patients and the cultured CRC cells. Moreover, the CRC cell-secreted miRNA N-72 could promote the migration, tubulogenesis, and permeability of endothelial cells. In addition, the mouse xenograft model was used to verify the facilitating effects of miRNA N-72 on CRC growth, angiogenesis, and metastasis in vivo. Further mechanism analysis revealed that CRC cell-secreted miRNA N-72 could be delivered into endothelial cells via exosomes, which then inhibited cell junctions of endothelial cells by targeting CLDN18 and consequently promoted angiogenesis. Our findings reveal a novel mechanism of CRC angiogenesis and highlight the potential of secreted miRNA N-72 as a therapeutic target and a biomarker for CRC.

Keywords: miRNA N-72, exosomes, colorectal cancer, angiogenesis, CLDN18

Introduction

The formation of new blood vessels and increased vascular permeability are critical for tumor metastasis [1, 2]. Although anti-angiogenesis is considered an important strategy in the treatment of colorectal cancer (CRC), the primary or acquired resistance toward anti-angiogenic drugs often causes therapeutic failure in some patients. Consequently, identifying a novel diagnostic marker and therapeutic target for anti-angiogenesis therapy in CRC is essential.

Studies have demonstrated that tumor cell-secreted microRNAs (miRNAs) play regulatory roles in tumor angiogenesis and metastasis [3, 4]. miRNA N-72, a novel miRNA, was confirmed to regulate EGF-induced migration by targeting MMP2 in human amnion mesenchymal stem cells (hAMSCs) [5]. However, the relation between miRNA N-72 and cancer remains unclear. Previously, to explore the regulatory relationship between miRNA N-72 and cancer, we collected and analyzed the expression of miRNA N-72 in the serum of patients with CRC and found that serum miRNA N-72 levels were higher in CRC patients than in healthy individuals. Therefore, this study aims to further investigate the role of miRNA N-72 in the development of CRC.

Exosomes are extracellular vesicles (diameter: 30-150 nm) with a double lipid layer [6, 7] that are widely found in cell culture supernatants and blood [8]. Tumor-secreted exosomes can mediate the intercellular communication between tumor and endothelial cells by delivering miRNA, thereby regulating tumor angiogenesis [9-11]. CRC cell-secreted exosomal miRNAs (microRNA-1246, miR-25-3p, and miR-21-5p) delivered into endothelial cells have been reported to regulate angiogenesis [12-14].

In this study, we detected miRNA N-72 in the serum of CRC patients and CRC cells. Additionally, CRC cell-secreted miRNA N-72 promoted the migration, permeability, and tube-forming ability of endothelial cells. Using mouse xenograft models, CRC cell-secreted miRNA N-72 was shown to facilitate tumor growth, angiogenesis, and metastasis of CRC in vivo. Further mechanistic investigations revealed that CRC cell-secreted miRNA N-72 could be delivered into endothelial cells via exosomes, which then inhibited cell junctions of endothelial cells by targeting and downregulating CLDN18 expression, thereby promoting tumor angiogenesis. This study disclosed a novel mechanism of angiogenesis in CRC, providing a basis for the potential use of miRNA N-72 as a biomarker and therapeutic target for CRC.

Materials and methods

Human CRC tissue specimens and serum samples of CRC patients

Serum samples and formalin-fixed, paraffin-embedded tissue specimens from colorectal cancer (CRC) patients who had received surgery without chemotherapy or radiotherapy were collected from the Affiliated Hospital of Jining Medical University. Serum samples were obtained from healthy donors (n = 10) and CRC patients (n = 20). The detailed information of healthy donors and CRC patients is provided in Tables S1 and S2, respectively. The CRC tissue samples (n = 135) were examined and confirmed by qualified pathologists. Then, the t*issue microarrays* with a diameter of 2.0 *mm* per core were constructed. Ethical approval was provided by the Ethics Committee of Jining Medical University Affiliated Hospital (Ethical approval number: 2021-11-B019), and informed *consent was obtai*ned from all participants.

Cell lines and cell culture

Human umbilical vein endothelial cells (HUVECs) were purchased from Beina Bio (Beijing, China) and cultured in endothelial cell medium (ECM, ScienceCell, USA). Subconfluent HUVECs at passages 3 to 5 were used in the experiments. Human CRC cell lines (SW620, HCT116, SW480, and HCT29) were provided by the American Type Culture Collection, and the mouse CRC cell lines (CT26 and MC38) were obtained from Beina Bio (Beijing, China). These cell lines were cultured in RPMI-1640 medium (GIBCO, Gaithersburg, USA) supplemented with 10% fetal bovine serum (FBS, BI, USA). The human intestinal epithelial cells (HIECs) were purchased from Nanjing Saihongrui Biotechnology Co., Ltd. (Nanjing, China) and cultured in high-glucose DMEM medium (GIBCO, Gaithersburg, USA) supplemented with 10% FBS. All cells were maintained in a humidified 5% CO_2 incubator at 37°C.

RNA oligoribonucleotides and cell transfection

miRNA N-72 mimics, mimic negative controls (mimics-NC), miRNA N-72 inhibitor (anti-N-72), inhibitor negative control (anti-NC), and Cy3-labeled miRNA N-72 were purchased from GenePharma (Shanghai, China). The RNA oligonucleotides were transfected into cells with Lipofectamine 3000 (Invitrogen, CA, USA).

Transwell migration assay

The migration ability of HUVECs was detected using 8-μm transwell chambers (Corning, USA). The HUVECs were suspended in serum-free medium and then added to the upper chamber. The culture medium with 10% FBS was added to the lower chamber. After 24 h, the migrated cells were fixed with 4% paraformaldehyde (PFA), stained with 0.1% crystal violet, and counted under the Olympus IX73 microscope (Olympus, Tokyo, Japan).

Tubule formation assay

Matrigel (BD Biosciences, USA) was added to 96-well plates and incubated at 37°C for 30 min to allow polymerization. The HUVECs passaged 3-5 times were harvested and seeded onto the Matrigel-coated 96-well plates, and the plates were then incubated in a 5% CO_2 incubator at 37°C. After 12 h, tube-like struc-

tures were observed and captured under the Olympus IX73 microscope (Olympus, Tokyo, Japan). Then, tubule formation was quantified using Image J software.

In vitro endothelial permeability assay

The HUVECs (1.0×10^5 cells/well) were seeded onto 0.4-μm transwell chambers to allow the formation of a confluent monolayer. Rhodamine-dextran (Sigma, USA) was added to the upper chamber and incubated for 30 min. Then, the culture medium from the lower chamber was collected, and fluorescence was measured at an excitation wavelength of 544 nm by using a Cytation 5 imaging reader (Biotek, VT, USA).

Cell counting kit 8 assay

The proliferation ability of HUVECs was evaluated using the cell counting kit 8 (CCK8) kit (Dojindo, Shanghai, China) according to the manufacturer's instructions. Briefly, after the HUVECs with different treatments were seeded onto a 96-well plate, 10 μL of CCK8 reagent was added to each well. Then, the HUVECs were incubated at 37°C for 1 h in a humidified incubator with 5% CO_2. The absorbance (optical density, OD) at 450 nm was measured to determine cell viability by using a microplate reader (Synergy H1 Hybrid Reader, BioTek, VT, USA).

Transendothelial invasion assay

The HUVECs (1×10^5 cells/well) were seeded in the upper chamber of a transwell insert, followed by the addition of phosphate-buffered saline (PBS) or SW620 cell-secreted exosomes (10 μg/mL). mCherry-labeled SW620 cells were then seeded onto the confluent monolayer of HUVECs for 24 h. The transmigrated SW620 cells in the bottom wells were counted under a fluorescence microscope (RVL-100-G, ECHO, San Diego, CA, USA).

Isolation, characterization, and quantification of exosomes

Exosomes were collected and purified from CRC cell-derived CM through ultracentrifugation. CM was obtained after 48 h of culture of CRC cells in serum-free medium, followed by centrifugation at 300×*g* for 10 min at 4°C, 2000×*g* for 10 min at 4°C, and 10000×*g* for 30 min at 4°C to remove cells and other debris. The final supernatants were filtered through a 0.22-μm filter (Millipore, MA, USA), and then, the supernatants were further ultracentrifuged at 100000×*g* for 70 min at 4°C to remove shedding and larger vesicles. The pellets were then washed with PBS and ultracentrifuged again at 100000×*g* for 70 min at 4°C. Next, exosomes were collected from pellets and resuspended in PBS. The exosomes were fixed with 2% PFA, placed on 200-mesh copper grids, and stained with 2% phosphotungstic acid for 2 min. Finally, the exosomes were viewed using a transmission electron microscope (TEM, Hitachi H-7500, Japan). Particle sizes of the exosomes were determined using ZetaView (Particle Metrix, Germany). The expressions of exosomal markers (CD9, CD63, CD81, and TSG101) were determined by western blotting. Exosome concentration was measured using the BCA protein assay kit (Beyotime, Shanghai, China).

Exosome uptake assays

To explore whether CRC cell-secreted exosomes can be taken up by endothelial cells, exosomes extracted from SW620 cells were labeled with the fluorescent membrane dye PKH67 (Sigma, St. Louis, MO, USA). Later, 2 μg of the labeled exosome was added to the cultured HUVECs and photographed at 0, 5, and 10 h using the fluorescence microscope (RVL-100-G, ECHO, San Diego, CA, USA).

To explore whether CRC cell-secreted exosomal miRNA N-72 can be delivered into endothelial cells, HUVECs were incubated for 48 h with exosomes from SW480 cells transfected with Cy3-labeled miRNA N-72. Then, the internalized fluorescence signals in the HUVECs were observed under a Zeiss LSM 800 laser confocal microscope (Zeiss, Oberkochen, Germany).

Real-time quantitative PCR

TRIzol reagent (Ambion, Austin, TX, USA) was used to extract total RNA from the cultured cells. The RevertAid First Strand cDNA Synthesis Kit (Thermo Scientific, MA, USA) was used to perform reverse transcription. Real-time quantitative PCR (qPCR) was performed on a CFX Connect Real-time System (Bio-Rad, Singapore) by using FastStart Universal SYBR Green Master (Rox) (Roche, Basel, Switzerland). The sequences of miRNA N-72 primers used are as follows: 5'-GCGTCTGTGAGCCACTCTC-3'

(forward) and 5'-GTGCAGGGTCCGAGGT-3' (reverse).

Western blotting analysis

Lysates of exosomes or the cultured cells were prepared using RIPA buffer (Beyotime, Shanghai, China) and quantified using the bicinchoninic acid assay (BCA assay). The lysates were subjected to SDS-PAGE and transferred onto the PVDF membrane (Millipore, MA, USA), followed by incubation with primary antibodies at 4°C overnight. The following primary antibodies were used: CD9 (Affinity, 1:2000 dilution), CD63 (Affinity, 1:2000 dilution), CD81 (Affinity, 1:2000 dilution), TSG101 (Affinity, 1:2000 dilution), claudin-18 (Proteintech, 1:2000 dilution), and β-actin (Affinity, 1:1000 dilution). After the incubation of the specific enzyme-labeled antibody (Jackson, 1:10000 dilution), chemiluminescent signals were detected using ECL detection reagents (Millipore, MA, USA).

Transcriptome sequencing and analysis

miRNA N-72 mimics- or mimics-NC-transfected HUVECs were collected for total RNA extraction. Transcriptome sequencing was performed at Berry Genomics Co., Ltd. (Beijing, China). RNA-seq libraries were constructed from total RNA (≥ 1 μg) by using the NEBNext® UltraTM RNA Library Prep Kit for Illumina® (NEB, USA) according to the manufacturer's protocol.

After library construction, the Qubit 2.0 Fluorometer was used for preliminary quantification, and the library was diluted to 1.5 ng/μL. Then, the insert size of the library was assessed using the Agilent 2100 bioanalyzer. After obtaining the expected insert size, the effective concentration of the library (> 2 nM) was quantified accurately through real-time quantitative PCR to ensure library quality. After the library met the desired quality, sequencing was performed on the Illumina platform, generating paired-end reads of 150 bp each.

Finally, differential expression analysis was performed using DESeq2 version 1.16.1, with two biological repeats for each group. GO and KEGG pathway enrichment analyses were performed using clusterProfiler (version 3.4.4).

Dual luciferase reporter assay

The wild-type or mutant CLDN18 luciferase reporter plasmid was obtained from GeneChem (Shanghai, China). The dual luciferase reporter assay was employed to determine whether miRNA N-72 targeted the 3'UTR of the CLDN18 gene. miRNA N-72 mimics or mimics-NC (50 nM each) and 200 ng of the firefly luciferase reporter plasmid containing the wild-type or mutant 3'UTR of the CLDN18 gene were co-transfected into HUVECs by using Lipofectamine 3000 (Invitrogen). Luciferase activities were measured using the dual luciferase reporter assay system (Beyotime, Shanghai, China) after 48 h of transfection.

Immunofluorescence analysis

miRNA N-72 mimics- or mimics-NC-transfected HUVECs were seeded onto coverslips in a 24-well plate. The cells were washed with PBS and fixed with 4.0% PFA for 15-20 min at room temperature and then blocked with 5% BSA for 30 min. The cells were incubated overnight at 4°C with the primary antibody (Claudin-18, 1:1000, Proteintech, China). Afterward, the cells were incubated with FITC-labeled secondary antibody (1:200, Earthox, USA) for 1 h at room temperature and protected from light. All cells were mounted with DAPI Fluoromount-G media (Southern Biotechnology, Alabama, USA). Immunofluorescence intensity was quantified using Image J software.

Establishment of CRC xenografts in mice

Female BALB/c mice (age: 6 weeks) were purchased from Jinan PengYue Laboratory Animal Breeding Co., Ltd. (Jinan, China), and the mice were maintained in a specific pathogen-free environment. All animal study protocols were approved by the Ethics Committee of The Affiliated Hospital of Jining Medical University (Ethical approval number: 2021-11-B019).

To explore whether miRNA N-72 can promote tumor growth and angiogenesis in vivo, 1×10^6 CT26 cells transfected with miRNA N-72 mimics or mimics-NC were subcutaneously injected into the BALB/c mice (5 mice/group) to establish the subcutaneous xenograft tumor model. The tumor volume was recorded on alternate days, and the tumors were resected and weighed 28 days after tumor inoculation.

To evaluate the effects of CRC cell-secreted exosomal miRNA N-72 on tumor growth and angiogenesis in vivo, the BALB/c mice were injected subcutaneously with 1×10^6 CT26

cells. On day 14 after tumor implantation, PBS (100 μL) or exosomes (10 μg in 100 μL PBS) derived from the anti-NC- or anti-N-72-transfected CT26 cells were injected into the tail vein of BALB/c mice (5 mice/group) on alternate days, and the tumor volumes were measured. After 14 days of treatment, tumors were resected and weighed.

For the model of experimental liver metastases, C57BL/6J mice were injected with 1×10^6 MC38 cells through the intrasplenic route [15]. PBS or exosomes derived from the anti-NC- or anti-N-72-transfected MC38 cells were injected into the tail vein of mice (5 mice/group). The mice were euthanized after 14 days, and the livers were resected to determine the number of hepatic metastatic foci. At the end of the experiment, all mice were euthanized with an overdose of carbon dioxide.

Fluorescence in situ hybridization assays

The paraffin-embedded human CRC tissues were cut into 4-μm sections for the subsequent fluorescence in situ hybridization (FISH) analysis. The miRNA N-72 fluorescent probes labeled with streptavidin-cyanin 3 (SA-Cy3) were obtained from GenePharma (Shanghai, China). The probe sequence was as follows: GCTCCAGAGAGTGGCTCACAGA.

miRNA N-72 probes (1 μM) were incubated with the tissue slides at 37°C for 12 h. The expression of miRNA N-72 in CRC tissues was detected using the Fluorescence In Situ Hybridization Kit (GenePharma, Shanghai, China) according to the manufacturer's instructions. The results were viewed under a Zeiss LSM 800 laser confocal microscope (Zeiss, Oberkochen, Germany).

Immunohistochemistry analysis

The paraffin sections were dewaxed, antigen repair was performed, and endogenous peroxidase was blocked. After blocking the sections in goat serum (Zhongshan Goldenbridge, China), the sections were incubated with the primary antibody (CD31, Abcam, 1:400 dilution) at 4°C overnight. Subsequently, the secondary antibody labeled with horseradish peroxidase was added to the sections and incubated at room temperature for 30 min, followed by staining with diaminobenzidine (DAB-0031, Maixi_Bio, Fuzhou, China) and hematoxylin (G1120, Solarbio, Beijing, China).

Tumor microvessel density (MVD) was assessed through immunohistochemical staining of CD31 as previously described [16]. First, the tissue sections were screened at a low power (5× magnification) to identify the areas of highest MVD (vascular hotspots). Then, the number of microvessels was counted in 5 randomized areas under higher magnification (400×), and the average value was calculated to represent MVD. Any CD31-positive cell or discrete cluster was counted as a single microvessel.

Statistical analysis

Statistical analysis was performed using GraphPad Prism version 8. All quantitative values are expressed as the mean ± SD. Independent samples *t*-test or one-way ANOVA was used to analyze differences among/between sample groups. Pearson correlation analysis was performed to determine correlations. A P value < 0.05 was considered statistically significant.

Results

Increased expression of miRNA N-72 in the CRC patients' serum and CRC cells

miRNA N-72 expression was measured in the serum samples from CRC patients and healthy volunteers. The results indicated that the miRNA N-72 expression in the serum from CRC patients was higher than that in healthy human sera (Figure S1A). Furthermore, a higher miRNA N-72 expression was detected in CRC cells than that in HUVECs and HIEC. Additionally, the miRNA N-72 expression was relatively higher in the two highly malignant CRC cell lines (SW620 and HCT116) and relatively lower in the CRC cell lines with lower malignancy (SW480 and HT29) (Figure S1B). These results indicate that the expression of miRNA N-72 can be detected in the serum of CRC patients as well as in cultured CRC cells.

CRC cell-secreted exosomes promote angiogenesis in vitro

Exosomes are known to deliver miRNAs to endothelial cells and regulate angiogenesis [9-11]. Therefore, we explored whether the CRC cell-secreted exosomes can regulate tumor

angiogenesis. Exosomes from the SW480 cells were extracted through ultracentrifugation and observed through TEM, which indicated that they exhibit cup- or sphere-shaped morphology (Figure S2A). In addition, the expression of exosome markers CD9, CD63, CD81, and TSG101 was detected in the extracted exosomes (Figure S2B). Diameters of the exosomes were measured through nanoparticle tracking analysis (NTA) and identified at 30-150 nm (Figure S2C).

To investigate whether the CRC cell-secreted exosomes can be taken up by HUVECs, the red fluorescent dye PKH26 was used to label exosomes derived from SW620 cells. The labeled exosomes were applied to HUVECs. As shown in **Figure 1A**, PKH26-labeled exosomes were observed within recipient HUVECs, suggesting that SW620 exosomes could be delivered into the HUVECs (**Figure 1A**). The transwell migration analysis showed that the number of migrated endothelial cells was increased after treatment with CRC cell-secreted exosomes (**Figure 1B**, **1C**). In the tube formation assay, the CRC exosome-transfected HUVECs showed a clear tube formation tendency (**Figure 1D**). A significant increase in the number of tubules (**Figure 1E**), number of branch junctions (**Figure 1F**) and vessel length (**Figure 1G**) was observed after treatment with CRC cell-secreted exosomes, suggesting that CRC exosomes could enhance the tube-forming ability of HUVECs. In vitro endothelial permeability assay was used to assess the traversing of rhodamine-labeled dextran through HUVEC monolayer that was non-treated or pre-treated with CRC cell-secreted exosomes. As shown in **Figure 1H**, pre-treatment with CRC cell-secreted exosomes allowed much more dextran to traverse through HUVEC monolayer, suggesting the increased permeability of the HUVEC monolayer.

CRC cell-secreted exosomal miRNA N-72 induces angiogenesis in vitro

To explore whether CRC cell-secreted miRNA N-72 plays a role in tumor angiogenesis, miRNA N-72 mimics and mimics-NC (a negative control for miRNA N-72 mimics) were transfected into SW480 cells. The miRNA N-72 transfection efficiency was assessed through RT-qPCR (**Figure 2A**). Exosomes from the miRNA N-72 mimics- or mimics-NC-transfected SW480 cells were collected and added to the cultured HUVECs for the subsequent experiments. According to the results of the CCK8 assays, exosomes from the miRNA N-72 mimics-transfected SW480 cells significantly enhanced the cell proliferation ability of HUVECs compared with that of the control group (HUVECs treated with exosomes from the mimics-NC-transfected SW480 cells) (**Figure 2B**). As shown in **Figure 2C**, the number of migrated HUVECs treated with exosomes from the miRNA N-72 mimics-transfected SW480 cells increased significantly compared with that of HUVECs treated with exosomes from the mimics-NC-transfected SW480 cells. Similarly, the tubule formation ability of HUVECs treated with exosomes from the miRNA N-72 mimics-transfected SW480 cells was higher than that of HUVECs treated with exosomes from the mimics-NC-transfected SW480 cells (**Figure 2D**). Next, the in vitro endothelial permeability assay was performed to measure the traversing of rhodamine-labeled dextran through the HUVEC monolayer treated with exosomes from the miRNA N-72 mimics- or mimics-NC-transfected SW480 cells. As shown in **Figure 2E**, more dextran traversed through the HUVEC monolayer pre-treated with exosomes from miRNA N-72-overexpressing SW480 cells, suggesting the increased endothelial permeability induced by exosomal miRNA N-72. The miRNA N-72 inhibitor (anti-N-72) or its negative control (anti-NC) was transfected into SW620 cells before isolating the exosomes from the culture medium. The transfection efficiency was assessed through RT-qPCR. As expected, the miRNA N-72 expression in exosomes from the anti-N-72-transfected SW620 cells was lower than that in exosomes from the anti-NC-transfected SW620 cells (**Figure 2F**). Then, exosomes from the anti-N-72 or anti-NC-transfected SW620 cells were co-cultured with HUVECs. Subsequent studies revealed that exosomes from the anti-N-72-transfected SW620 cells reduced the cell proliferation (**Figure 2G**), migration (**Figure 2H**), tubulogenesis (**Figure 2I**), and permeability (**Figure 2J**) of HUVECs compared with those from the anti-NC-transfected SW620 cells. These results showed that CRC cell-secreted exosomal miRNA N-72 could promote angiogenesis of HUVECs.

Angiogenesis regulation effects of CRC cell-secreted exosomes depend on miRNA N-72 expression in endothelial cells

To investigate whether CRC cell-secreted exosomes depend on miRNA N-72 expression in

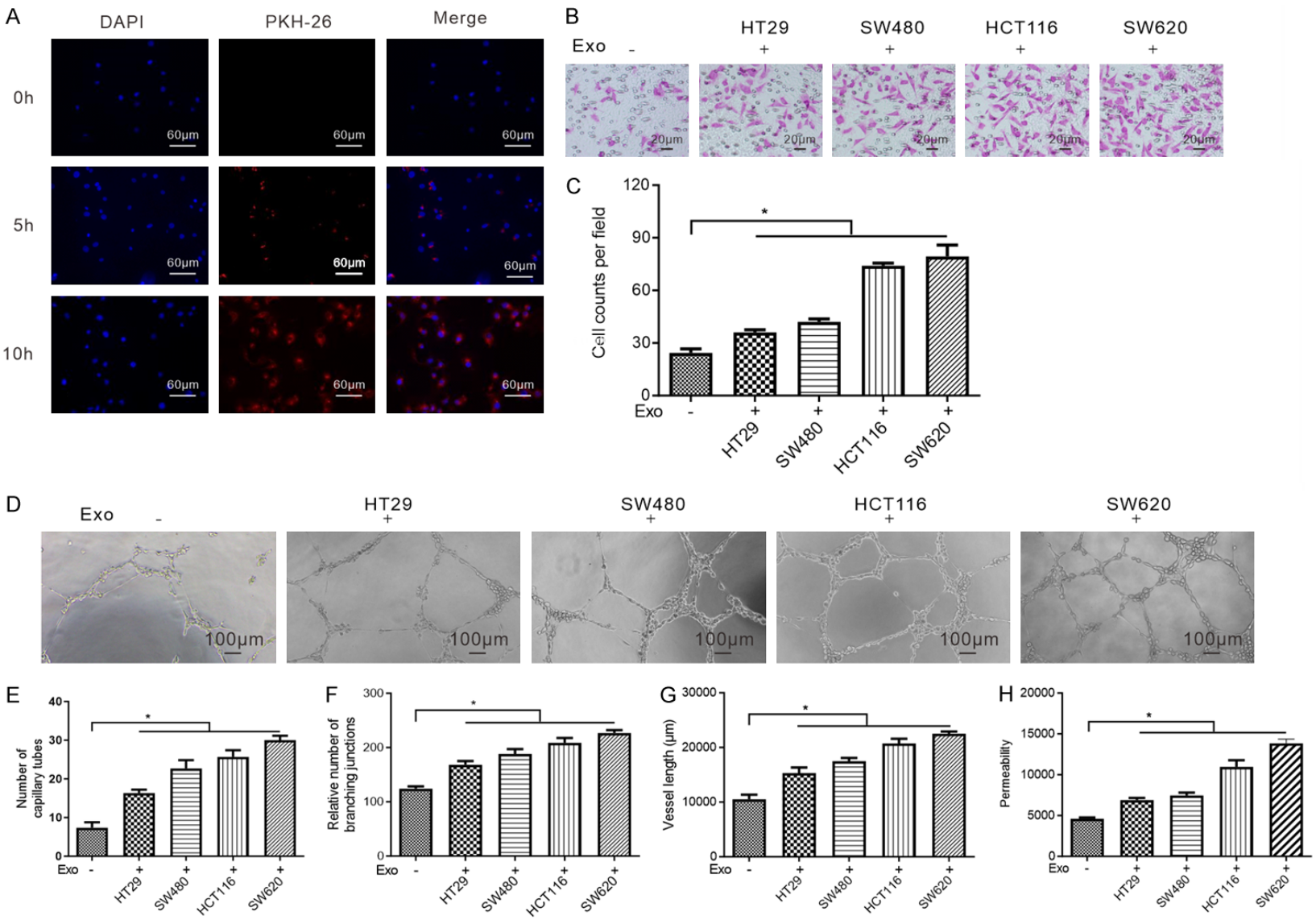

Figure 1. Regulatory effects of CRC cell-secreted exosomes on angiogenesis in vitro. A. Exosomes from SW620 cells that were labeled with PKH26 were applied to treat HUVECs, following by imaging under a fluorescence microscope at 0, 5, and 10 h. HUVECs and exosomes were stained with DAPI and PKH26, respectively. B, C. Effect of CRC cell-secreted exosomes on the migration ability of HUVECs. D-G. Effect of CRC cell-secreted exosomes on the tube-forming ability of HUVECs. H. Effect of CRC cell-secreted exosomes on the monolayer endothelial permeability. All experiments were repeated three times. Data are shown as the mean ± SD. * represents $P < 0.05$.

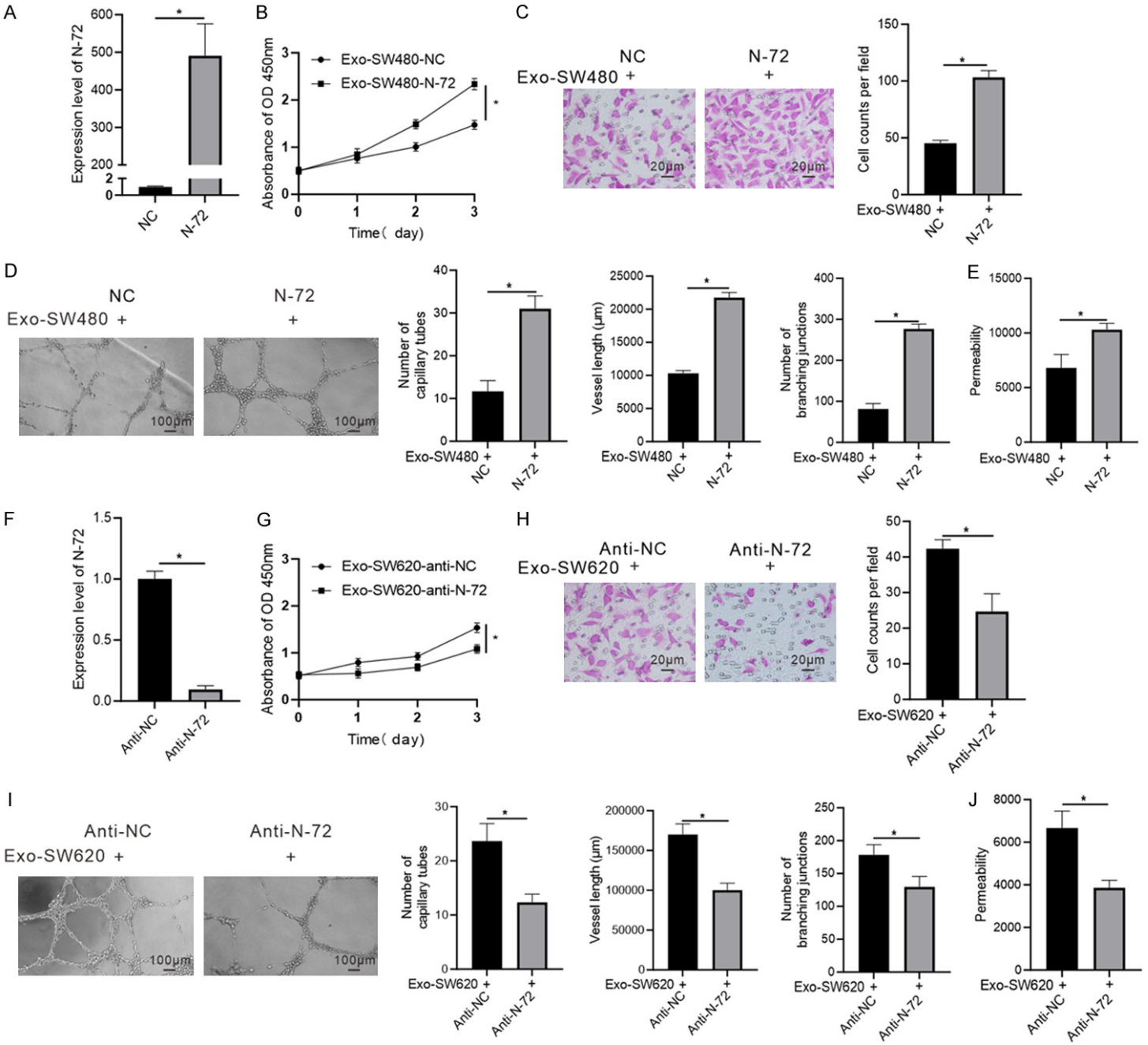
A
Expression level of N-72
NC
N-72
B
Absorbance of OD 450nm
Exo-SW480-NC
Exo-SW480-N-72
Time(day)
C
NC
N-72
Exo-SW480 +
20μm
Cell counts per field
D
100μm
Number of capillary tubes
Vessel length (μm)
Number of branching junctions
E
Permeability
F
Anti-NC
Anti-N-72
G
Exo-SW620-anti-NC
Exo-SW620-anti-N-72
H
Exo-SW620 +
I
J

Figure 2. Effects of CRC cell-secreted exosomal miRNA N-72 on angiogenesis in vitro. A. miRNA N-72 expression in exosomes from the mimics-NC- or miRNA-N-72-transfected SW480 cells was detected through RT-qPCR. B. CCK8 assays indicated that HUVECs treated with exosomes from the miRNA N-72 mimics-transfected SW480 cells significantly enhanced the cell proliferation ability of HUVECs compared with that of the control group (HUVECs treated with exosomes from the mimics-NC-transfected SW480 cells). C. The migration ability of HUVECs treated with exosomes from the mimics-NC- or miRNA-N-72-transfected SW480 cells was observed using the transwell migration assay. D. The tubule-formation ability of HUVECs treated with exosomes from the mimics-NC- or miRNA-N-72-transfected SW480 cells. E. HUVEC monolayer that was pre-treated with exosomes from the miRNA-N-72-transfected SW480 cells displayed increased permeability. F. RT-qPCR analysis of miRNA N-72 expression in the exosomes from the anti-N-72- or anti-NC-transfected SW620 cells. G. Cell proliferation ability was determined using CCK8 assay. HUVECs were treated with exosomes from the anti-N-72- or anti-NC-transfected SW620 cells. The absorbance was detected at 0, 24, 48 and 72 h. H. The migration ability of HUVECs was determined using the transwell assay after the cells were treated with exosomes from the anti-N-72- or anti-NC-transfected SW620 cells. I. The tubule-formation ability of HUVECs was observed using the tubule formation assay after the HUVECs were treated with exosomes from the anti-N-72- or anti-NC-transfected SW620 cells. J. The in vitro endothelial permeability assay was conducted to measure the traversing of rhodamine-dextran through the HUVEC monolayer treated with exosomes from the anti-N-72- or anti-NC-transfected SW620 cells. All experiments were repeated three times. Data shown are the mean ± SD. * represents $P < 0.05$.

endothelial cells to exert regulatory effects on angiogenesis, we conducted the transwell migration assay, tubule formation assay, and transendothelial invasion assay.

Anti-N-72- or anti-NC-transfected HUVECs were treated with or without the exosomes from SW620 cells. As shown in **Figure 3A**, more HUVECs migrated out of the inserts after the treatment with SW620 cell-secreted exosomes, whereas antagonizing endogenous miRNA N-72 in HUVECs attenuated the promoting ability of SW620 cell-secreted exosomes. Furthermore, the tubule formation assay confirmed that the tubule length, number of tubules, and number of tubule branches of the HUVECs pretreated with SW620 cell-derived exosomes increased, and the above enhancing effects were attenuated after endogenous miRNA N-72 knockdown in HUVECs (**Figure 3B**). The transendothelial invasion assay indicated that more SW620 cells invaded through HUVEC monolayers pretreated with SW620 cell-secreted exosomes, and this enhanced transendothelial invasion was weakened by antagonizing endogenous miRNA N-72 within HUVECs. The aforementioned results suggested that CRC cell-secreted exosomes increased the permeability of HUVEC monolayers depending on endogenous miRNA N-72 expression in the HUVECs (**Figure 3C**).

CRC cell-secreted miRNA N-72 is delivered to endothelial cells through exosomes

We then explored whether exosomes mediated the transfer of miRNA N-72 from CRC cells to endothelial cells. RT-qPCR results showed that miRNA N-72 expression significantly increased in the HUVECs incubated with the CRC cell-secreted exosomes (Figure S3A). miRNA N-72 expression in the recipient HUVECs significantly decreased after the cells were incubated with exosomes from the anti-N-72-transfected SW620 cells (Figure S3B). Consistently, as shown in Figure S3C, RT-qPCR results indicated significantly reduced miRNA N-72 expression in the recipient HUVECs after the cells were incubated with the exosomes derived from SW620 cells treated with the exosome inhibitor (GW-4869). Next, HUVECs were treated with exosomes from SW480 cells transfected with Cy3-labeled miRNA N-72. miRNA N-72-Cy3 fluorescence was observed within the recipient HUVECs (Figure S3D). The aforementioned results suggested that the exosomes derived from SW480 cells mediated the transfer of miRNA N-72 into endothelial cells.

miRNA N-72 promotes tumor growth and angiogenesis of CRC xenografts

To explore whether miRNA N-72 can promote tumor growth and angiogenesis of CRC in vivo, miRNA N-72 mimics- or mimics-NC-transfected CT26 cells were subcutaneously injected into the back of BALB/c mice to establish a subcutaneous CRC model. Compared with xenografts originating from the mimics-NC-transfected CT26 cells, xenografts originating from the miRNA N-72-transfected CT26 cells displayed increased tumor volume (**Figure 4A**, **4B**) and tumor weight (**Figure 4C**). More neoplastic cells infiltrated into the surrounding tissue in xenografts originating from the miRNA N-72-

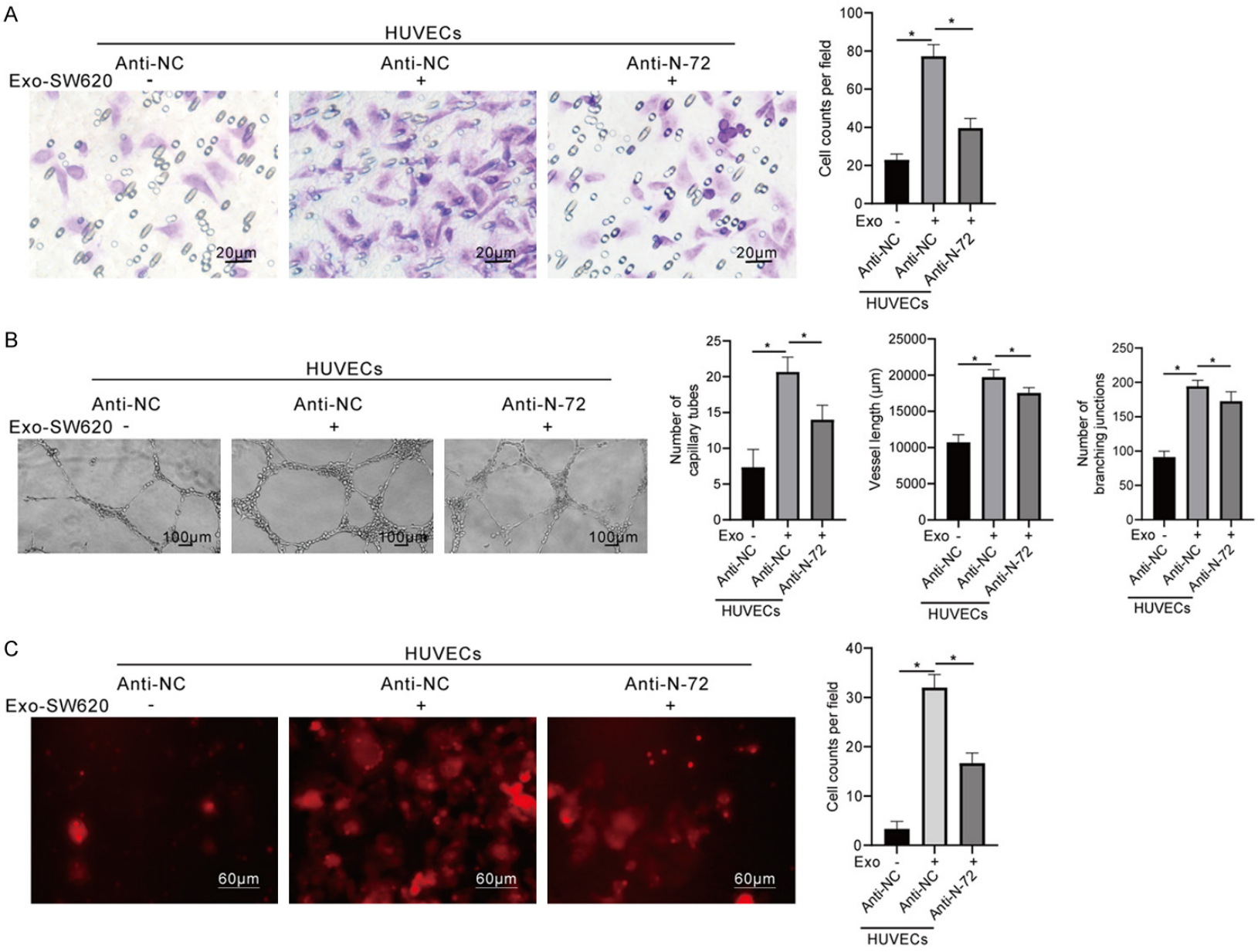
A
HUVECs
Anti-NC
Anti-NC
Anti-N-72
Exo-SW620 -
+
+
20μm
20μm
20μm
Cell counts per field
100
80
60
40
20
0
Exo - + +
Anti-NC
Anti-NC
Anti-N-72
HUVECs
B
HUVECs
Anti-NC
Anti-NC
Anti-N-72
Exo-SW620 -
+
+
100μm
100μm
100μm
Number of capillary tubes
25
20
15
10
5
0
Vessel length (μm)
25000
20000
15000
10000
5000
0
Number of branching junctions
250
200
150
100
50
0
Exo - + +
Anti-NC
Anti-NC
Anti-N-72
HUVECs
C
HUVECs
Anti-NC
Anti-NC
Anti-N-72
Exo-SW620 -
+
+
60μm
60μm
60μm
Cell counts per field
40
30
20
10
0
Exo - + +
Anti-NC
Anti-NC
Anti-N-72
HUVECs

Figure 3. Antagonizing endogenous miRNA N-72 attenuated the ability of CRC cell-secreted exosomes to regulate angiogenesis. For (A-C), HUVECs were transfected with anti-NC or anti-N-72 for 24 h and then cultured with or without exosomes derived from SW620 cells. (A) Antagonizing endogenous miRNA N-72 in HUVECs attenuated the capacity of SW620 cell-derived exosomes to increase migration ability. HUVEC monolayer was cultured on the transwell filter without (-) or with exosomes (+) for 48 h, and the number of migrated cells in the lower chamber was detected through transwell migration assay. (B) The tube-forming ability of HUVECs with different treatments was evaluated through the tubule formation assay. Antagonizing endogenous miRNA N-72 attenuated the ability of SW620 cell-secreted exosomes to enhance the tube-forming ability of HUVECs. (C) The transendothelial invasion assay was performed to detect the endothelial monolayer permeability. Antagonizing endogenous miRNA N-72 attenuated the ability of SW620 cell-secreted exosomes to increase the transendothelial invasion of cancer cells. Anti-N-72- or anti-NC-transfected HUVECs were seeded on transwell inserts and incubated with SW620 cell-secreted exosomes for 48 h. MCherry-labeled SW620 cells were added to the top of pre-treated HUVEC monolayer and incubated for 24 h, and then, the mCherry-labeled cells that passed through the HUVEC monolayer were counted. All experiments were repeated three times. Data shown are the mean ± SD. * represents $P < 0.05$.

transfected CT26 cells than in xenografts originating from the mimics-NC-transfected CT26 cells (**Figure 4D**). Furthermore, higher MVD was observed in the xenografts originating from the miRNA N-72-transfected CT26 cells (**Figure 4E**, **4F**). These results suggested that miRNA N-72 could promote the growth, invasion, and angiogenesis of CRC in the mice xenograft model.

CRC cell-secreted exosomal miRNA N-72 promotes angiogenesis, tumor growth, and metastasis of CRC xenografts

We next evaluated the effects of CRC cell-secreted exosomal miRNA N-72 on angiogenesis, tumor growth, and metastasis by using the mouse xenograft model. BALB/c mice were injected subcutaneously with CT26 cells. Exosomes were collected from the anti-NC- or anti-N-72-transfected CT26 cells. Next, 14 days after tumor implantation, PBS and exosomes derived from the anti-NC- or anti-N-72-transfected CT26 cells were injected into BALB/c mice through the tail vein every other day for 14 days. The tumor volumes were measured at the same time. The exosome-treated tumors exhibited increased growth (**Figure 5A**, **5B**) and weight (**Figure 5C**) and higher MVD than the PBS-treated tumors (**Figure 5D**, **5E**). The aforementioned promoting effects of exosomes from CRC cells were attenuated after miRNA N-72 knockdown in the exosomes (**Figure 5A-E**).

To further evaluate the effects of exosomal miRNA N-72 on metastasis in vivo, MC38 cells were injected into the spleen of mice to establish a mouse model of liver metastasis. Exosomes were collected from the anti-NC- or anti-N-72-transfected MC38 cells and then injected into the mice via the tail vein; PBS was injected into the control mice. Two weeks later, the mice were euthanized and their livers were resected. As shown in **Figure 5F-H**, the extent of liver metastasis in the exosome (transfected with anti-NC)-treated mice increased compared with that in the PBS-treated mice, indicating the metastasis-promoting effects of the CRC cell-derived exosomes. Moreover, the promoting effects of the exosomes could be significantly attenuated after miRNA N-72 knockdown. These results indicated that exosomal miRNA N-72 derived from the CRC cells promoted tumor growth, angiogenesis, and metastasis.

CRC cell-secreted exosomal miRNA N-72 reduces endothelial cell junction integrity by targeting CLDN18

The aforementioned data demonstrated the tumor angiogenesis-promoting effects of miRNA N-72 from CRC-derived exosomes. To further explore the underlying molecular mechanism, transcriptome sequencing of HUVECs with miRNA N-72 overexpression was performed. As shown in Figure S4A, 401 genes were upregulated and 129 genes were downregulated in miRNA N-72-overexpressing HUVECs. Among the downregulated genes in N-72-overexpressing HUVECs, 7 genes (*SHROOM4, MARVELD3, CLDN2, LAMA4, CLDN18, VEGFD,* and *EGF*) were associated with the tight junctions between cells (Figure S4B). The KEGG pathway analysis indicated that the tight junction pathway was significantly enriched (Figure S4C).

To determine the target gene of miRNA N-72, miRanda software was used to predict the possible downstream target genes, and 3220 possible target genes were screened. By overlapping these screened target genes with the 129 downregulated genes obtained through tran-

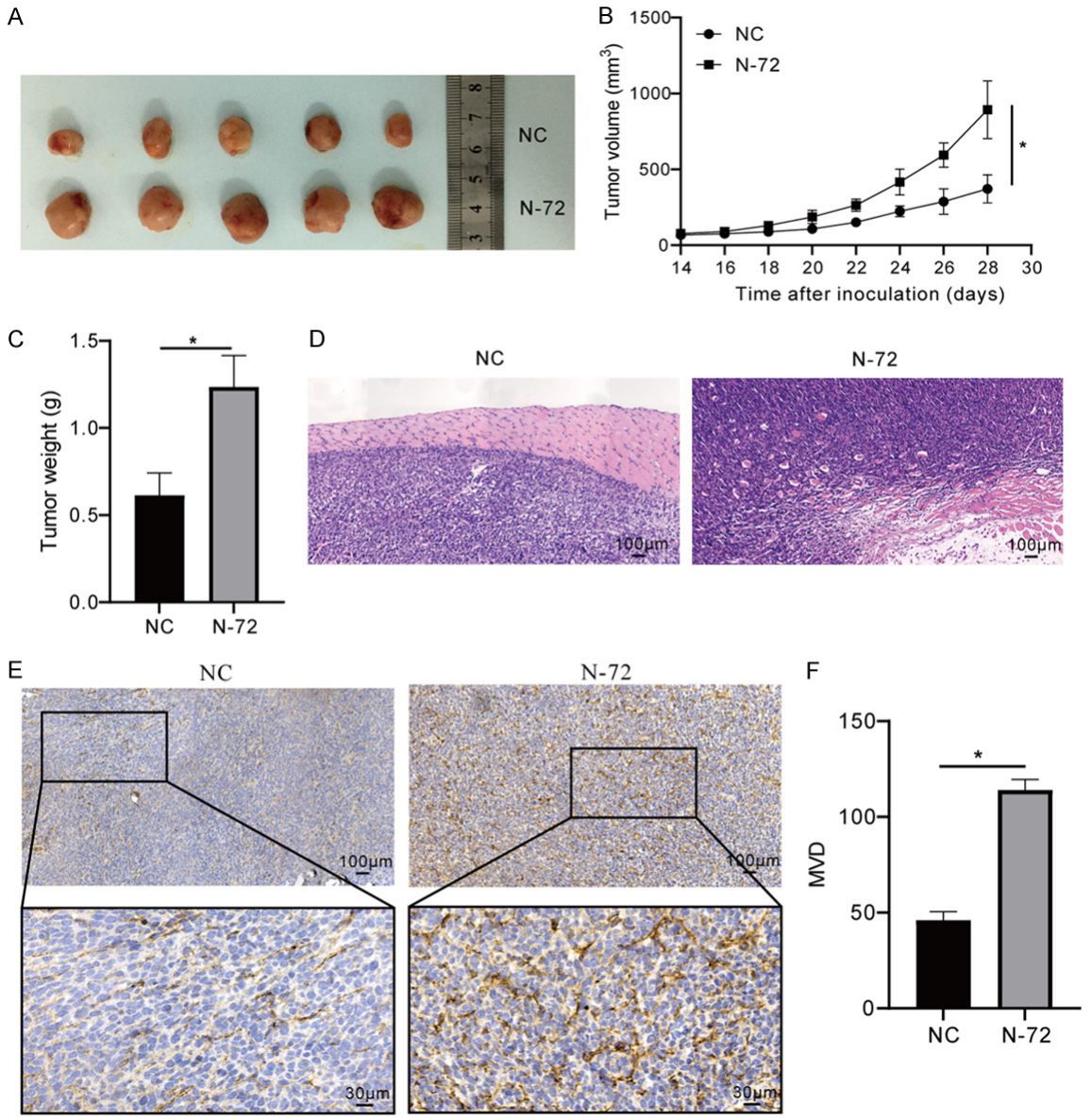

Figure 4. miRNA N-72 induced growth and angiogenesis in the CRC xenograft model. A. Representative images of the resected tumors from the CRC implanted mouse model. B. Tumor volume curve of the transplanted tumors with different miRNA N-72 expressions. C. Tumor weight of the CRC xenografts with different miRNA N-72 expressions. D. H&E-stained xenograft tissues showing the infiltration of tumor cells into the surrounding subcutaneous tissues. E. Representative images of CD31-stained xenograft tissues. F. MVD of the xenograft tissues with different miRNA N-72 expressions.

scriptome sequencing analysis, 19 target genes were intersected (Figure S4D). Then, tight junction-related genes (*MARVELD3* and *CLDN18*) among the 19 selected genes were used for subsequent verification through RT-qPCR. The results showed that CLDN18 expression significantly decreased in miRNA N-72-overexpressing cells (Figure S5A, S5B). To evaluate the correlations between CLDN18 and miRNA N-72, the expressions of miRNA N-72 and CLDN18 in the HUVEC, HIEC and CRC cells were determined, and the correlation analysis was performed. The results showed that the miRNA N-72 levels were negatively correlated with the levels of CLDN18, as with an increase in miRNA N-72 levels, CLDN18 levels tended to decrease (correlation coefficient $r = -0.8876$, $P < 0.05$, Figure S5C).

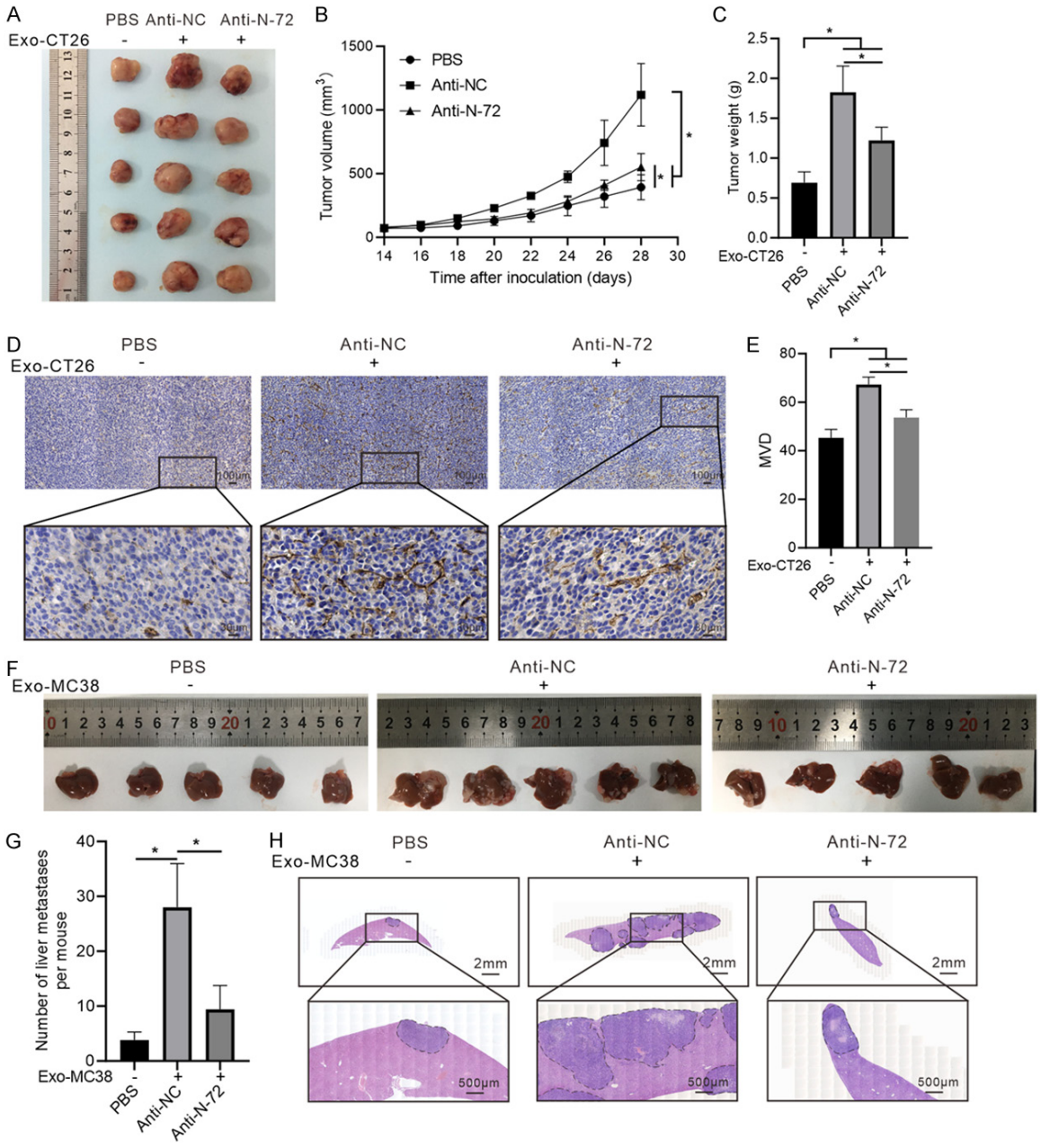

Figure 5. CRC cell-secreted exosomal miRNA N-72 promotes tumor angiogenesis, growth, and metastasis in the CRC transplanted mouse model. A. Representative images of the harvested tumors. B. Tumor volume curve of CRC xenografts with different treatments. C. Tumor weight of the xenografts. D. CD31 expression was examined in tumor tissues from mice after various treatments. E. MVDs were quantified. F and G. Representative images and the quantification of liver metastasis foci from the mouse metastasis model. H. H&E-stained liver tissues from the mouse liver metastasis model. Data shown are the mean ± SD. * represents $P < 0.05$.

The potential binding site between CLDN18 and miRNA N-72 was identified using the TargetScan database (http://www.targetscan.org; **Figure 6A**). Then, the dual-luciferase reporter assay was performed to validate the binding between miRNA N-72 and CLDN18. As shown in **Figure 6B**, in the wild-type group, the luciferase activity was significantly decreased in the miRNA N-72 mimics-transfected cells compared with the mimics-NC-transfected cells. In addition, no significant difference was observed in the luciferase activity following transfection with miRNA N-72 mimics in the mutant group, which did not contain the pre-

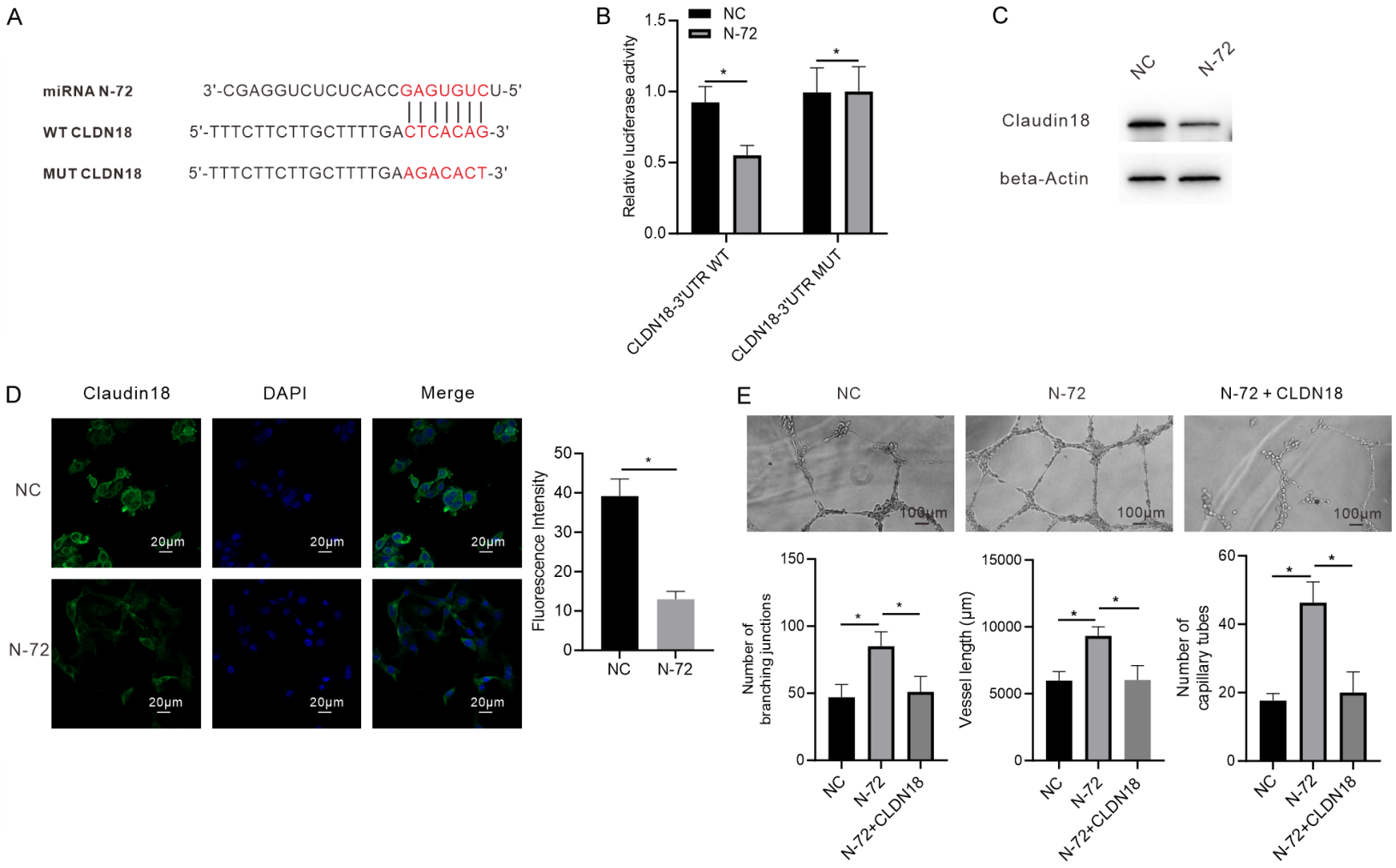
A
miRNA N-72 3'-CGAGGUCUCUCACCGAGUGUCU-5'
WT CLDN18 5'-TTTCTTCTTGCTTTTGACTCACAG-3'
MUT CLDN18 5'-TTTCTTCTTGCTTTTGAAGACACT-3'
B
NC
N-72
Relative lucferase activity
1.5
1.0
0.5
0.0
CLDN18-3'UTR WT
CLDN18-3'UTR MUT
C
NC
N-72
Claudin18
beta-Actin
D
Claudin18
DAPI
Merge
NC
N-72
20μm
Fluorescence Intensity
50
40
30
20
10
0
NC
N-72
E
NC
N-72
N-72 + CLDN18
100μm
Number of branching junctions
150
100
50
0
Vessel length (μm)
15000
10000
5000
0
Number of capillary tubes
60
40
20
0
NC
N-72
N-72+CLDN18

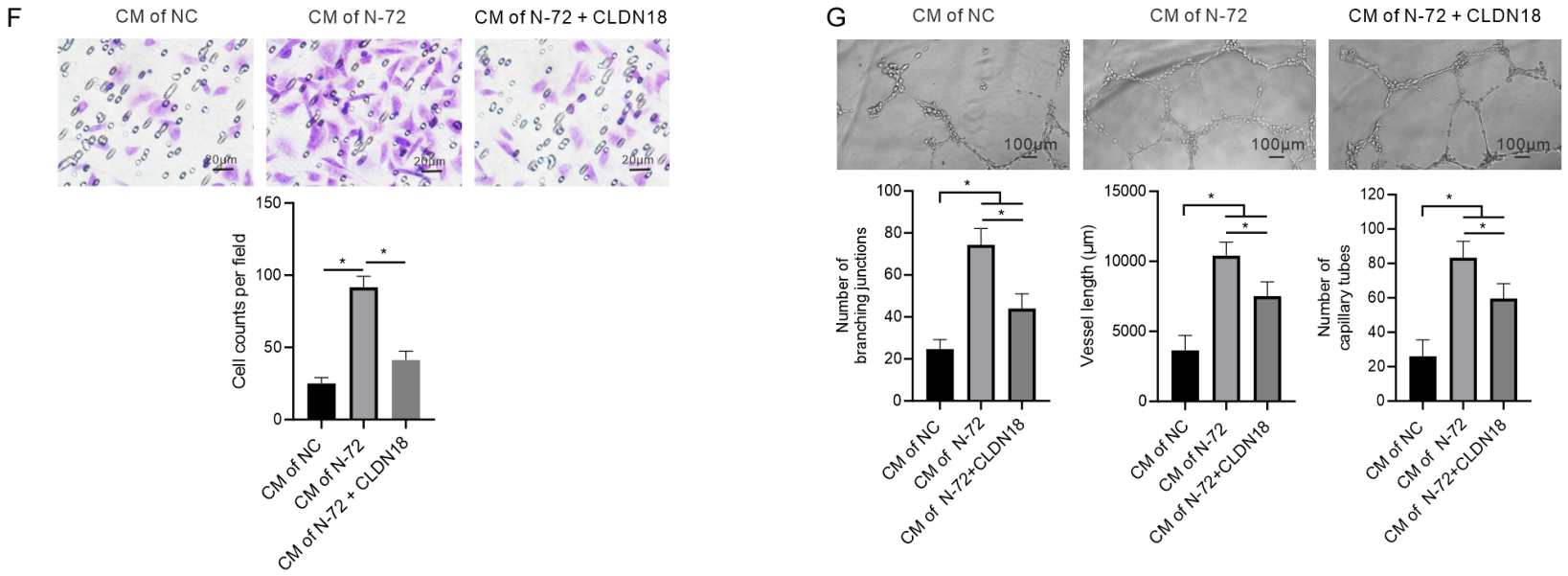

Figure 6. Regulatory effects of miRNA N-72 on CLDN18 expression. A. Predicted binding sites of miRNA N-72 within the 3'UTR of CLDN18. B. Relative luciferase activities of HUVECs subjected to co-transfection of miRNA N-72 mimics with firefly luciferase reporter plasmid that contained WT or mutant CLDN18 3'-UTR. C. Western blotting analysis of CLDN18 expression in miRNA N-72 mimics- or mimics-NC-transfected HUVECs. D. CLDN18 expression in miRNA N-72 mimics- or mimics-NC-transfected HUVECs was detected through IF analysis. The fluorescence signal showed that the claudin-18 protein (encoded by CLDN18) was localized in the cell membrane. E. Tubule formation assay for HUVECs transfected with mimics-NC or miRNA N-72 or co-transfected with miRNA N-72 and CLDN18 overexpression plasmid. The number of tubes, branching junctions, and the vessel length were determined. F, G. CM from the miRNA N-72 mimics- or mimics-NC-transfected SW480 cells was collected 48 h after transfection and then added to the cultured HUVECs with or without CLDN18 overexpression. F. HUVEC monolayer was cultured on the transwell filter with CM for 48 h, and the number of migrated cells in the lower chamber was determined through transwell migration assay. G. The tube-forming ability of HUVECs subjected to different treatments was evaluated through the tubule formation assay. Data shown are the mean ± SD. * represents $P < 0.05$.

dicted binding sites. To further verify whether CLDN18 is a functional target gene of miRNA N-72, HUVECs were transfected with miRNA N-72 or mimics-NC, and then CLDN18 expression was determined through western blotting and IF analysis. As shown in **Figure 6C**, **6D**, the CLDN18 expression was significantly downregulated after miRNA N-72 overexpression in the HUVECs, indicating that CLDN18 may be a target of miRNA N-72. To confirm that miRNA N-72 reduced endothelial cell junction integrity, thereby promoting tumor angiogenesis, by targeting CLDN18, the HUVECs were transfected with mimics-NC or miRNA N-72 or co-transfected with miRNA N-72 and CLDN18 overexpression plasmid for tubule formation assay. As shown in **Figure 6E**, after transfection of HUVECs with miRNA N-72, the tubule formation ability was enhanced, as evidenced by the increased number of tubes, branching junctions, and the vessel length. Notably, the enhanced effects were reversed by CLDN18 overexpression. Collectively, the exosomal miRNA N-72 derived from CRC cells reduced endothelial cell junction integrity by targeting CLDN18. In order to further validate the role of miRNA N-72 in promoting tumor angiogenesis through targeting CLDN18, we transfected miRNA N-72 mimics and mimics-NC into SW480 cells. Subsequently, we collected the conditioned medium (CM) from the miRNA N-72 mimics- or mimics-NC-transfected SW480 cells and added it to cultured HUVECs with or without CLDN18 overexpression. As depicted in **Figure 6F**, the migration ability of HUVECs was enhanced upon transfection of SW480 cells with miRNA N-72. Importantly, the augmented effects of miRNA N-72 were significantly mitigated when CLDN18 was overexpressed in HUVECs. Moreover, the tubule formation assay validated that the treatment of HUVECs with CM from SW480 cells overexpressing miRNA N-72 resulted in increased tubule length, number of tubules, and number of tubule branches. These enhancing effects were attenuated upon CLDN18 overexpression in HUVECs (**Figure 6G**). These findings collectively indicate the reliance of CLDN18 expression for the angiogenesis-promoting effects of miRNA N-72.

miRNA N-72 expression in human CRC tissues

To explore the expression and clinicopathological significance of miRNA N-72 in CRC tissues, FISH staining of miRNA N-72 was performed using human CRC tissues. The results showed that miRNA N-72 expression was relatively higher in the tumor cells than in the normal intestinal epithelial cells (Figure S6).

Discussion

Angiogenesis is a crucial player in tumor growth and metastasis [1], but the exact mechanism of CRC angiogenesis remains unclear and the drugs targeting tumor angiogenesis have not been sufficiently efficacious for CRC. Therefore, it is of great significance to explore the mechanism of angiogenesis in CRC and develop the corresponding targeted drugs. Recent studies have demonstrated that CRC cell-secreted miRNA might exert a pro-angiogenic effect in CRC by regulating the intercellular communication between CRC cells and endothelial cells [12-14].

miRNA N-72 is a new miRNA that was first reported in hAMSCs [5] and was shown to regulate EGF-induced hAMSC migration by targeting MMP2. However, the relation between miRNA N-72 and cancer remains unclear. In this study, high miRNA N-72 expression was detected in the serum of CRC patients, indicating that miRNA N-72 may be used as an early non-invasive diagnostic biomarker for CRC. The study also showed that CRC cell-secreted exosomal miRNA N-72 could be delivered into endothelial cells, which can promote the migration, tubulogenesis, and permeability of those endothelial cells. Moreover, miRNA N-72 was found to promote tumor angiogenesis, growth, and metastasis of CRC xenografts. In addition, we found that miRNA N-72 could exert pro-angiogenic effects by targeting *CLDN18*, which encodes the claudin-18 protein belonging to the claudin family of tight junction proteins [17, 18], and these proteins are essential for the formation of tight junctions in the epithelial and endothelial cells [19]. Inter-endothelial cell junctions are critical for the maintenance of vascular integrity [20, 21], and junctional complexes comprise tight junctions, adherens junctions, and gap junctions [22]. A recent study demonstrated that the exosomal miR-103 secreted by hepatoma cells could be delivered into endothelial cells, which inhibited the expression of junctional proteins VE-Cad, p120-catenin (p120), and ZO-1, thereby disrupting endotheli-

al junction integrity and increasing vascular permeability, consequently promoting tumor metastasis [9]. Similarly, breast cancer cell-secreted miR-105 could be delivered into endothelial cells and could disrupt the vascular endothelial cell barrier by suppressing ZO-1 and promoting metastasis [11]. This study reports for the first time a novel miRNA secreted by CRC cells to regulate tumor angiogenesis by targeting the tight junction protein CLDN18. The study provides a basis for the potential application of secretory miRNA N-72 as a predictive diagnosis marker and treatment target for CRC.

Acknowledgements

This study was funded by the National Natural Science Foundation of China (81972629), the Taishan Scholars Program of Shandong Province (tsqn201909193), Shandong Youth Innovation and Technology program (2020KJL-003), Research Fund for Academician Lin He New Medicine (JYHL2021FMS15), Shandong Medical and Health Science and Technology Development Plan Project (202104080301) and Jining Research and Development Program (2021YXNS074).

Disclosure of conflict of interest

None.

Address correspondence to: Yan-Rong Liu, Department of Pathology, Affiliated Hospital of Jining Medical University, Jining Medical University, No. 89 Guhuai Road, Jining 272029, Shandong, China. E-mail: liuyanrong1984@163.com

References

[1] Carmeliet P and Jain RK. Molecular mechanisms and clinical applications of angiogenesis. Nature 2011; 473: 298-307.

[2] Reymond N, d'Agua BB and Ridley AJ. Crossing the endothelial barrier during metastasis. Nat Rev Cancer 2013; 13: 858-870.

[3] Tang XR, Wen X, He QM, Li YQ, Ren XY, Yang XJ, Zhang J, Wang YQ, Ma J and Liu N. MicroRNA-101 inhibits invasion and angiogenesis through targeting ITGA3 and its systemic delivery inhibits lung metastasis in nasopharyngeal carcinoma. Cell Death Dis 2017; 8: e2566.

[4] Lu Y, Qin T, Li J, Wang L, Zhang Q, Jiang Z and Mao J. MicroRNA-140-5p inhibits invasion and angiogenesis through targeting VEGF-A in breast cancer. Cancer Gene Ther 2017; 24: 386-392.

[5] Li Y, Zhang D, Chen M, Wang R, Zhang T, Zhao F, Lin X and Pang X. The novel miRNA N-72 regulates EGF-induced migration of human amnion mesenchymal stem cells by targeting MMP2. Int J Mol Sci 2018; 19: 1363.

[6] Colombo M, Raposo G and Thery C. Biogenesis, secretion, and intercellular interactions of exosomes and other extracellular vesicles. Annu Rev Cell Dev Biol 2014; 30: 255-289.

[7] Kowal J, Tkach M and Thery C. Biogenesis and secretion of exosomes. Curr Opin Cell Biol 2014; 29: 116-125.

[8] Vlassov AV, Magdaleno S, Setterquist R and Conrad R. Exosomes: current knowledge of their composition, biological functions, and diagnostic and therapeutic potentials. Biochim Biophys Acta 2012; 1820: 940-948.

[9] Fang JH, Zhang ZJ, Shang LR, Luo YW, Lin YF, Yuan Y and Zhuang SM. Hepatoma cell-secreted exosomal microRNA-103 increases vascular permeability and promotes metastasis by targeting junction proteins. Hepatology 2018; 68: 1459-1475.

[10] Zhou Z, Zhang H, Deng T, Ning T, Liu R, Liu D, Bai M, Ying G and Ba Y. Exosomes carrying microRNA-155 target forkhead box O3 of endothelial cells and promote angiogenesis in gastric cancer. Mol Ther Oncolytics 2019; 15: 223-233.

[11] Zhou W, Fong MY, Min Y, Somlo G, Liu L, Palomares MR, Yu Y, Chow A, O'Connor ST, Chin AR, Yen Y, Wang Y, Marcusson EG, Chu P, Wu J, Wu X, Li AX, Li Z, Gao H, Ren X, Boldin MP, Lin PC and Wang SE. Cancer-secreted miR-105 destroys vascular endothelial barriers to promote metastasis. Cancer Cell 2014; 25: 501-515.

[12] Yamada N, Tsujimura N, Kumazaki M, Shinohara H, Taniguchi K, Nakagawa Y, Naoe T and Akao Y. Colorectal cancer cell-derived microvesicles containing microRNA-1246 promote angiogenesis by activating Smad 1/5/8 signaling elicited by PML down-regulation in endothelial cells. Biochim Biophys Acta 2014; 1839: 1256-1272.

[13] Zeng Z, Li Y, Pan Y, Lan X, Song F, Sun J, Zhou K, Liu X, Ren X, Wang F, Hu J, Zhu X, Yang W, Liao W, Li G, Ding Y and Liang L. Cancer-derived exosomal miR-25-3p promotes pre-metastatic niche formation by inducing vascular permeability and angiogenesis. Nat Commun 2018; 9: 5395.

[14] He Q, Ye A, Ye W, Liao X, Qin G, Xu Y, Yin Y, Luo H, Yi M, Xian L, Zhang S, Qin X, Zhu W and Li Y. Cancer-secreted exosomal miR-21-5p induces angiogenesis and vascular permeability by targeting KRIT1. Cell Death Dis 2021; 12: 576.

[15] Arabzadeh A, McGregor K, Breton V, Van Der Kraak L, Akavia UD, Greenwood CMT and Beauchemin N. EphA2 signaling is impacted by carcinoembryonic antigen cell adhesion molecule 1-L expression in colorectal cancer liver metastasis in a cell context-dependent manner. Oncotarget 2017; 8: 104330-104346.
[16] Weidner N, Semple JP, Welch WR and Folkman J. Tumor angiogenesis and metastasis--correlation in invasive breast carcinoma. N Engl J Med 1991; 324: 1-8.
[17] Zhang WH, Zhang SY, Hou QQ, Qin Y, Chen XZ, Zhou ZG, Shu Y, Xu H and Hu JK. The significance of the CLDN18-ARHGAP fusion gene in gastric cancer: a systematic review and meta-analysis. Front Oncol 2020; 10: 1214.
[18] Li J, Zhang Y, Hu D, Gong T, Xu R and Gao J. Analysis of the expression and genetic alteration of CLDN18 in gastric cancer. Aging (Albany NY) 2020; 12: 14271-14284.
[19] Otani T and Furuse M. Tight junction structure and function revisited. Trends Cell Biol 2020; 30: 805-817.
[20] Dejana E, Tournier-Lasserve E and Weinstein BM. The control of vascular integrity by endothelial cell junctions: molecular basis and pathological implications. Dev Cell 2009; 16: 209-221.
[21] Herbert SP and Stainier DY. Molecular control of endothelial cell behaviour during blood vessel morphogenesis. Nat Rev Mol Cell Biol 2011; 12: 551-564.
[22] Wallez Y and Huber P. Endothelial adherens and tight junctions in vascular homeostasis, inflammation and angiogenesis. Biochim Biophys Acta 2008; 1778: 794-809.

Table S1. The age and gender information of healthy donors

ID	Age	Gender
1	46	Female
2	32	Female
3	70	Female
4	36	Female
5	50	Male
6	50	Male
7	57	Male
8	30	Male
9	46	Male
10	55	Female

Table S2. The age and gender information of CRC patients

ID	Age	Gender
1	74	Male
2	73	Female
3	75	Male
4	63	Male
5	78	Male
6	77	Female
7	51	Female
8	72	Male
9	61	Male
10	68	Female
11	82	Female
12	61	Female
13	54	Male
14	73	Male
15	54	Male
16	64	Male
17	66	Female
18	57	Male
19	80	Male
20	69	Male

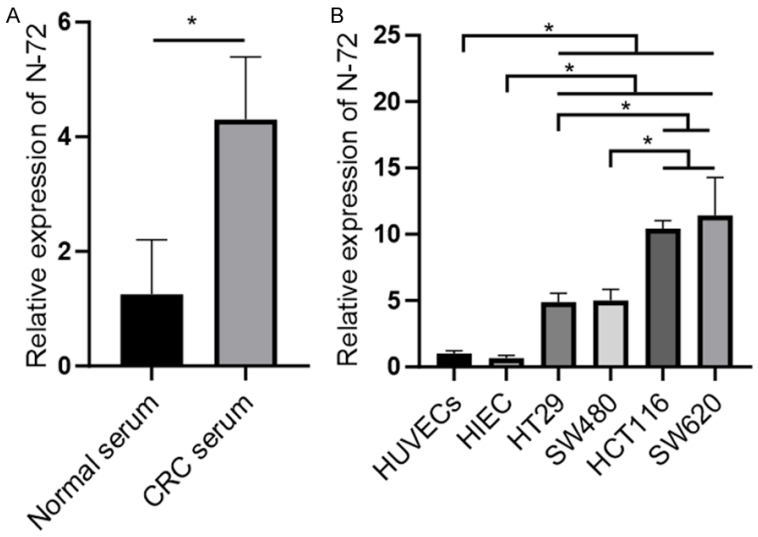

Figure S1. Detection of miRNA N-72 in serum of CRC patients and CRC cells. A. RT-qPCR analysis of the miRNA N-72 expression level in healthy human sera and the serum of CRC patients. B. RT-qPCR analysis of the miRNA N-72 expression level in HUVECs, HIEC and CRC cells. All experiments were repeated three times. Data shown are mean ± SD. * represented $P < 0.05$.

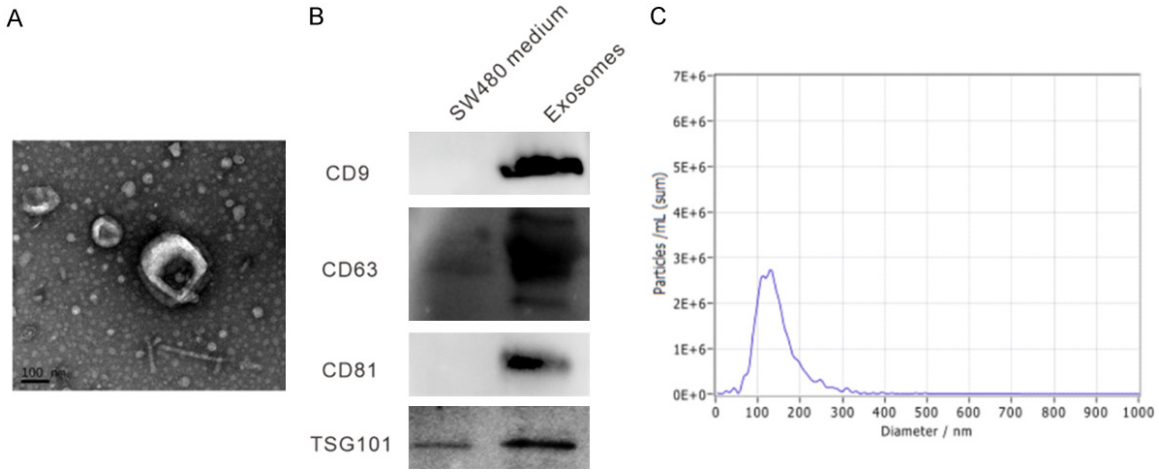

Figure S2. Isolation and validation of exosomes extracted from CRC cells. A. Morphology of exosomes extracted from SW480 cells observed under TEM. B. Western blotting analysis of exosome markers including CD9, CD63, CD81, and TSG101. C. The particle size distribution of the exosomes extracted from SW480 cells, as assessed through NTA analysis.

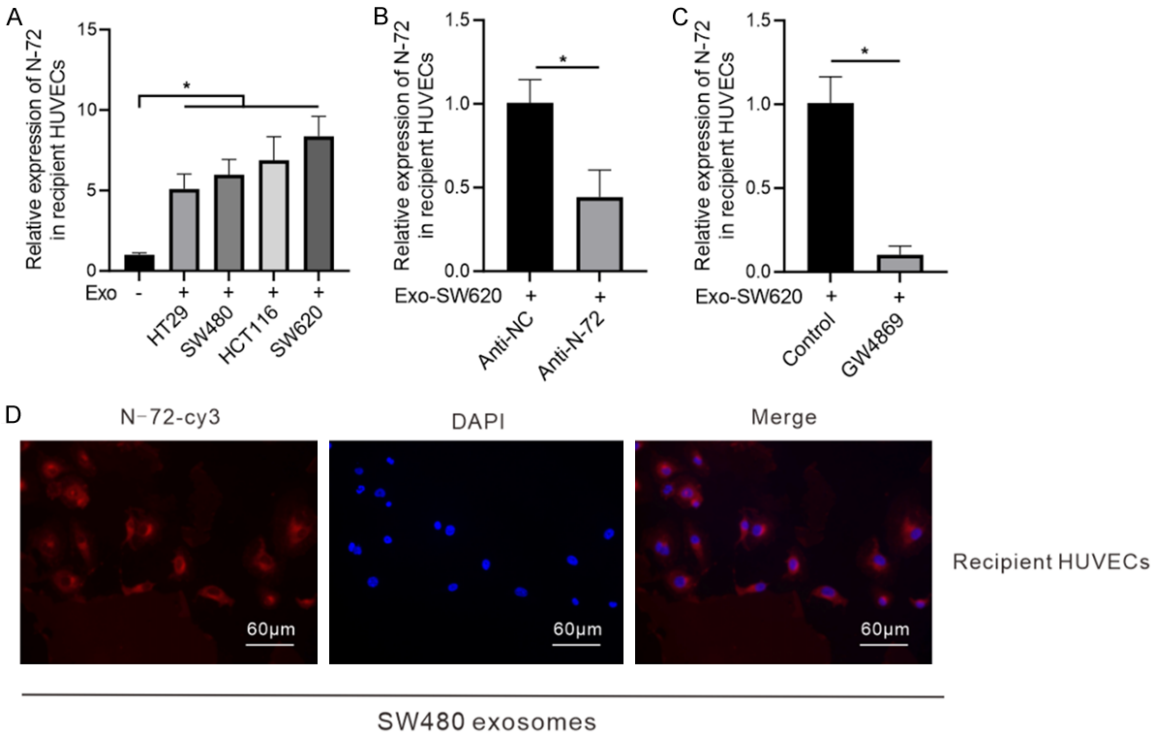

Figure S3. CRC cell-secreted exosomes mediate the delivery of miRNA N-72 into endothelial cells. A. miRNA N-72 expression increased in recipient HUVECs co-incubated with exosomes derived from different CRC cells. B. miRNA N-72 expression was decreased in recipient HUVECs cultured with exosomes derived from or anti-N-72-transfected SW620 cells. C. The miRNA N-72 expression in recipient HUVECs co-incubated with exosomes derived from SW620 cells treated with or without GW4869 was detected through RT-qPCR. Blocking exosome secretion of SW620 cells attenuated the miRNA N-72 level in the recipient HUVECs. D. Exosomes were prepared from SW480 cells transfected with Cy3-labeled miRNA N-72, followed by co-incubation with HUVECs in the transwell device. The fluorescence signal of Cy3-labelled miRNA N-72 in HUVECs was observed through confocal microscopy. All experiments were repeated three times. Data shown are mean ± SD. * represented $P < 0.05$.

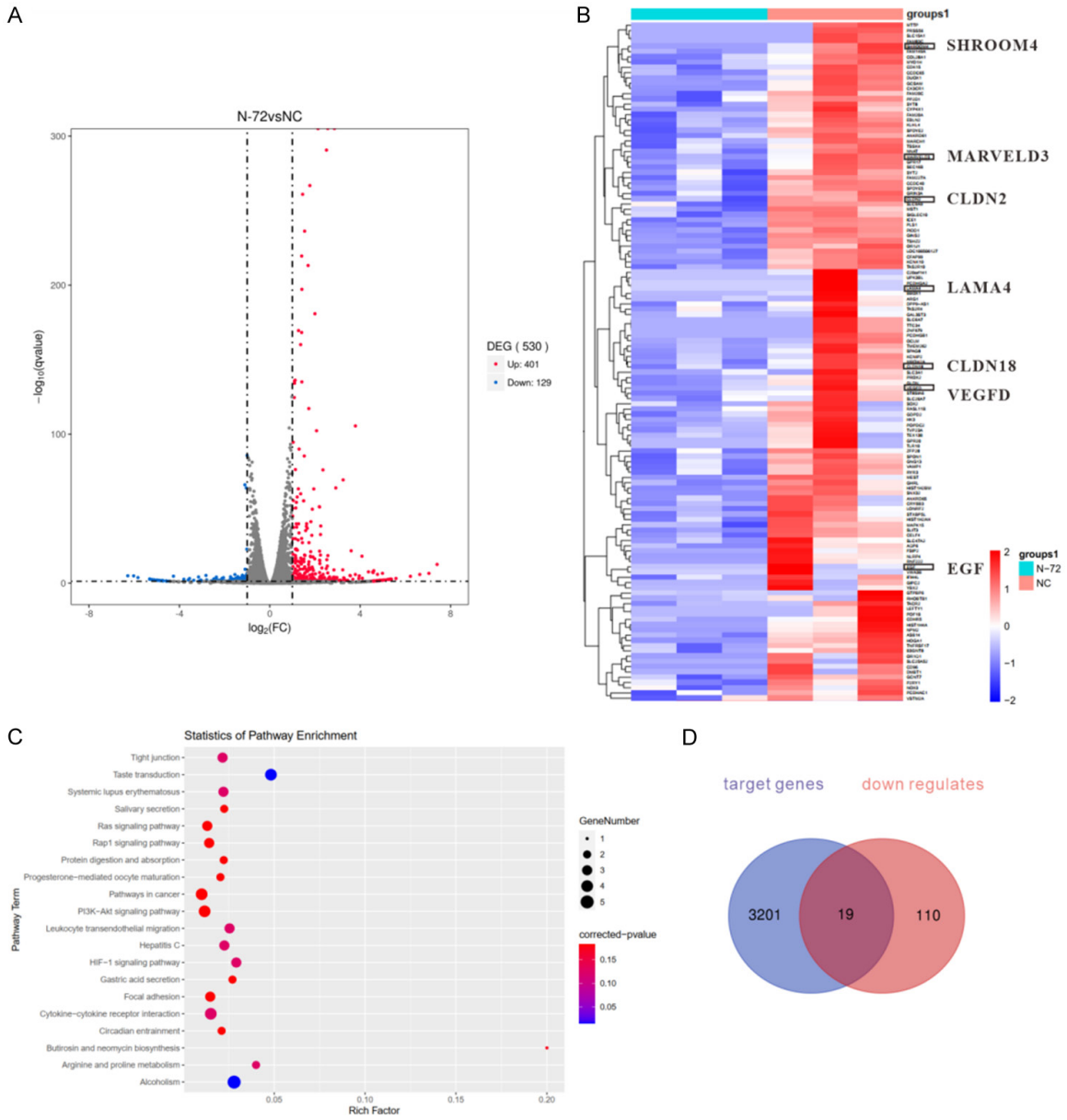

Figure S4. Transcriptome sequencing of HUVECs with different expression of miRNA N-72. A. Volcano plot analysis of differential expression genes consisting of 401 upregulated genes and 129 downregulated genes. B. Heatmap of the differential expression genes in mimics-NC- or miRNA N-72 mimics-transfected HUVECs. C. KEGG pathway analysis of differential expression genes. D. A Venn diagram showing the overlap between the predicted target genes analyzed through miRanda and the downregulated genes obtained through transcriptome sequencing analysis.

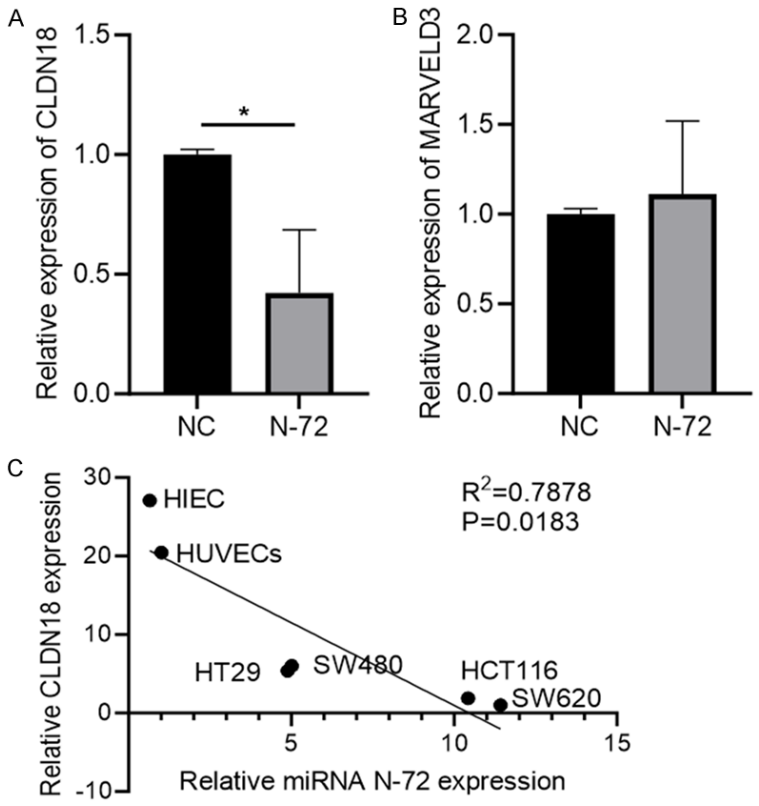

Figure S5. RT-qPCR analysis of the two tight junction-related genes. RT-qPCR validation of CLDN18 expression (A) and MARVELD3 expression (B) in miRNA N-72 mimics- or mimics-NC-transfected HUVECs. (C) The correlations between CLDN18 and miRNA N-72. Data shown are mean ± SD. * represented $P < 0.05$.

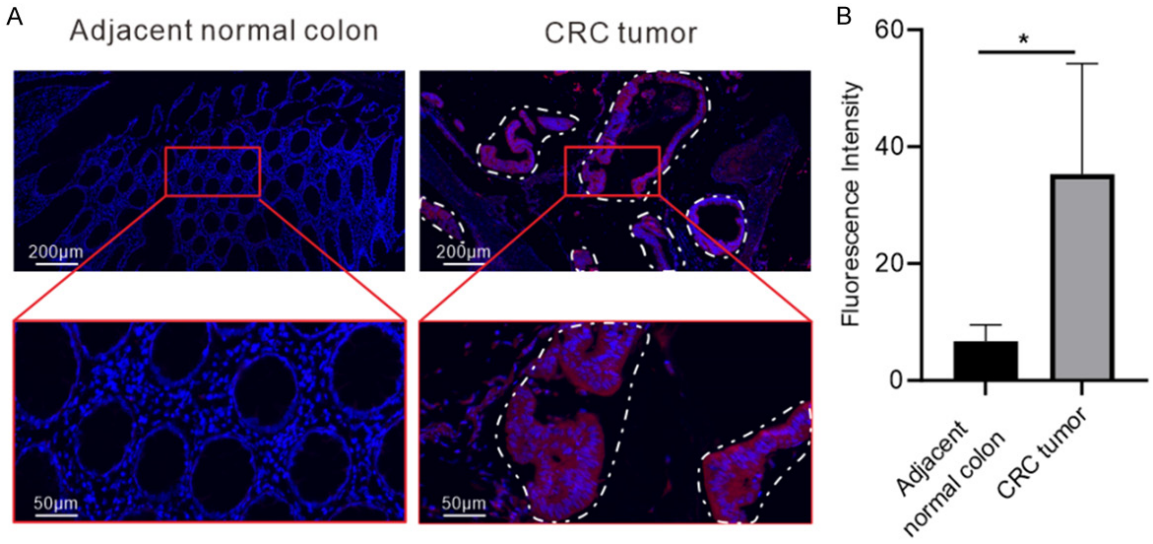

Figure S6. miRNA N-72 expression in human CRC tissue. A. Representative images of miRNA N-72 expression in human CRC and the adjacent normal colon tissues detected by FISH staining. B. Quantification of FISH staining of miRNA N-72 in human CRC and the adjacent normal colon tissues. Data shown are mean ± SD. * represented $P < 0.05$.